A Heuristic Approach to Dynamic Stiffness Control

Farhad Fakour
K. N. Toosi University of Technology
M. Hossein Siadati (siadati@kntu.ac.ir)
K. N. Toosi University of Technology https://orcid.org/0000-0003-2347-1246

Research Article

Keywords: Static/dynamic stiffness control, Mass participation factor, Finite element analysis, Weight reduction

Posted Date: December 8th, 2021

DOI: https://doi.org/10.21203/rs.3.rs-1101272/v1

Abstract

For appropriate and even superior performance yet cost reduction, this work was performed with the aim of weight reduction in the overall design and construction of possibly any machine tools. As far as our literature search is concerned, there does not seem to be much work published regarding successful weight reduction while maintaining performance using mass participation factor (MPF) in the areas of interest of the machine tools. In order to accomplish this task, we started with the 'bed' compartment of a CNC system and resorted to using the finite element analysis (FEA) software package and thoughtfully manipulated the available data/parameters until the desired results were obtained. The most important parameters were static stiffness, dynamic stiffness, and damping ratio. On the 'bed' of the machines' compartment currently in production, it was so identified that there was unnecessary material (dead weight), and thus the FEA software was used in order to remove the unnecessary material by iteration. Finally, a new machine was built devoid of the unnecessary material, resulted in 9.3% weight reduction as predicted by the simulation, without sacrificing any accuracy and/or precision in performance.

Highlights

- The aim is weight reduction in the overall design and construction of possibly any machine tools.
- The finite element analysis (FEA) software package was used to simulate weight reduction using mass participation factor (MPF) in the areas of interest while maintaining performance.
- The simulation was first applied to the 'bed' compartment, and then extended to the entire machine.
- Based on the simulation results, a new machine was constructed.
- Finally, the same pieces were machined using both the new and the production machines, and observed that the new machine with 9.3% reduced weight performed just as well as the production machine.

Introduction

Considering the importance of smooth and precise manufacturing, there have been continuous attempts in upgrading machine tools for enhancing their performance, weight reduction, and of course, cost minimization. Various aspects of optimization have been considered such as computer-aided engineering [1] or genetic algorithm [2], or grey relational analysis [3], or by load-bearing topology [4] or even by a biologically inspired topology optimization method [5], and also on static and dynamic characteristics [6–8], for lathe-bed [9, 10] or vertical milling machines [11, 12]. Also, weight reduction by using composite materials (13), or by shape optimization using static stiffness optimization have been considered [14]. However, very few attempts have focused on using mass participation factor (MPF) to achieve machine optimization [15, 16]. The mathematics of MPF has also been reported [17], however, to the best of our

knowledge, no attempt has been undertaken to compare the simulation results to the experimental results.

In this study, we used MPF in the areas of interest of a machine currently in *production* to minimize/eliminate the unnecessary material (dead weight) in constructing a *new* machine. Indeed, a *new* machine with 9.2% less weight was constructed based on the simulation results, and the iterations involved. For this purpose, the following activities were conducted.

Fea Static Analysis

Static Stiffness

For start, a model was created in the Solid Modeler software. Then, to analyze the model, it was transferred to the FEA software. During the analysis, the model was first constrained from some specific sites on the model (constraint sites) as shown with color green in Fig. 1.

Then forces in the X-axis were applied onto some specific areas of the constrained model to obtain the ratio of force over deflection in order to determine the static stiffness in the X-axis for each specific area a force was applied. The same was applied in the Y-axis, and then to the Z-axis followed by determining the static stiffness for each specific area the force was applied.

Fea Modal Analysis

Unconstrained Modal Analysis

The structure may contain a number of local modes in vibration, and identifying them is of great importance (16). The first few modes are called rigid modes (translational). The rigid modes have extremely low frequency and are of not much interest in this study. It is important to note that the first twisting mode is of special interest in this heuristic technique due to the inherent occurrence of its frequency and modal shape. The first twisting mode is also known as non-rigid mode. Of considerable importance is the fact that this twisting mode is at the center of gravity whose MPF is the least as shown with blue color in the *bed* of the *production* machine (Fig. 2). In the complex system of machine tools, the bed is a very important part because its layout and dimensions affect the dynamic performance of the entire machine (16).

On the other hand, the areas with the largest MPF are shown with red color in Fig. 2. It is important to note that MPF involves the mass that causes vibration with some frequency (23 Hz). In other words, the MPF associated with each mode represents the amount of system mass participating in that mode. If the value associated with MPF is small, it indicates that there is little vibration in that particular area, and vice versa.

Constrained Modal Analysis

The same constraints as in the static analysis apply in this section, too. The constraint sites as presented in green color, along with the first 5 modes and their corresponding MPF are shown in Fig. 3. The scheme of the original simulated model ('bed' compartment currently in *production*, referred to as the *production bed* here on) is shown in Fig. 3a, and Fig. 3b shows the new simulated model (the bed with weight reduction, referred to as the *new bed* here on). The darker blue in Fig. 3b illustrates the first twisting mode; it is superior for its smaller amplitude.

The frequencies and modal shapes of the first 5 modes are important; the first mode being the most important. Among these five, the first mode inherently has the lowest frequency (144 Hz, Fig. 3a). The challenge is to modify by iterations, and thus to minimize the MPF of the first mode in the areas of interest on the *new bed* (151 Hz Fig. 3b). It is important to note that the localities of the areas of interest remain the same throughout the entire simulation.

Furthermore, the MPF minimization at areas of interest will be achieved without sacrificing the static stiffness in all 3 axes. At the same time, we have succeeded in reducing or minimizing the mass of the part/machine. For instance, in this study, the total mass reduction for the part in Fig. 3 is 9%. Along with mass reduction, achieving the least MPF is desirable because it shows the best characteristics of the created/developed model. In a similar MPF simulation study, by raising the natural frequency, the weight of the bed was reduced by 4.8% (16).

Fea Dynamic Analysis

Harmonic Analysis

In order to study the dynamic stiffness, harmonic analysis was performed. While the information provided by dynamic analysis are displacement, velocity, and acceleration, in this study, we were interested in studying the displacement only. It is known that the results from harmonic analysis confirm the effects of MPF at any particular area of interest by studying the amplitude of dynamic displacement. The size of amplitude determines the magnitude of dynamic stiffness at any particular mode; the smaller the amplitude, the larger the dynamic stiffness. As shown in Fig. 4, the graphs compare the frequencies and amplitudes of the first modes for both the *production* and *new* models. It is obvious that the brown dash graph describing the *new* model shows a smaller amplitude at the first mode. Another important point is the fact that the two graphs are at different frequencies indicating better damping and dynamic stiffness for the *new* model. It is important to note that the same constraints and also 10% of the forces (same direction) as in the static analysis were applied in this harmonic analysis. Knowing that the smallest static stiffness is the worst, the harmonic analysis was done in the axis that showed the smallest static stiffness.

Experimental

Dynamic and modal tests were conducted to verity the simulation results. In order to do the tests, a ‘bed’ compartment based on the size and dimensions resulted by the *new* model was built. The *new* model was 9.3% (605 lb.) lighter than the *production* model. For comparison purposes, the experimental tests were conducted on both the *production* and the *new* ‘bed’ compartments.

Dynamic Tests

Both ‘bed’ compartments were tested using **two different** test methods, the shaker test, and the modal (hammer) test.

Shaker Test on the ‘bed’ compartment

For conducting the shaker test, a powerful centrifugal shaker was placed on the ‘bed’ compartment where the ‘column’ compartment sits. The amplitude and frequency of the vibrations experienced at four different sites on each linear guide at equidistant places from each other were captured by tri-accelerometer sensors. The software LabVIEW was used for data acquisition/analysis. As shown in Fig. 5, the shaker and the two accelerometers attached to the left and right of the ‘bed’ compartment onto the contact surface of the linear guides are observed. The other three measurements were conducted by placing the accelerometers farther away from the ‘column’ compartment. It is important to note that each accelerometer captures vibrations in time domain of 10 seconds experienced in all 3 axes simultaneously.

Modal (Hammer) Test on the ‘bed’ compartment

For this test, a hammer was used to exert a force on a particular area of the ‘bed’ compartment and measure the vibration along the same axis as the force was exerted. In other words, when the force was exerted in the X-axis, the vibration in the X-axis was measured. Accelerometers were used for measuring the vibration. This was done identically for both ‘bed’ compartments, but the accelerometers were placed only on the left-hand side of the ‘bed.’ One accelerometer was used at a time and measured the vibrations in all 3 axes. The complete procedure for this test involving data acquisition/analysis was done using Data Physics software/hardware.

Resutls And Discussion

Shaker test results

Figure 6 shows the vibration graphs for the left and the right linear guides of the *production bed* and the *new bed* in all 3 axes, as numerically presented in Table 1. The crucial features to observe in Figure 6 are the variations, in gravity unit (g = 9.81 m^2/s), within the 3 axes as well as those in-between the two beds (*production* and *new*). For the *production bed*, as shown in Figure 6a, the red and blue graphs illustrate the left side and the right side, respectively. One obvious point is the fact that MPF is large in both X and Y axes, while in the Z-axis, it is mostly low amplitude and thus not considerable. For instance, in Figure 6a

and Table 1a, the variations in the X-axis from the left (0.016 g) to the right (0.018 g) linear guides indicate that they are not identically the same. This fact is also evident in the frequency domain (20 Hz) of the Fast Fourier Transform (FFT) graphs in root mean square (RMS) values, 0.01130 vs. 0.01150, as shown in Table 1b.

Furthermore, the improvement in the g values in-between the *production bed* and the *new bed* can also be observed. For instance, as shown in Table 1a, the variations in the Y-axis are (0.013 and 0.005) for the left side, and (0.025 and 0.010) for the right side; the improvement (more damping) is 0.008 and 0.015 for the left and the right sides, respectively. Moreover, the FFT values (Table 1b) indicate the same trend for the Y-axis at 20 Hz; (0.00780 and 0.00280) and (0.01200 and 0.00400) for the left and the right sides of the two beds; the improvement is 0.005 and 0.008 for the left and the right sides, respectively.

In order to compare the variations with more ease, Fig. 7 shows the variations superimposed in one graph for each side; the red and blue are for the *production bed*, onto which the white and green for the *new bed* are superimposed. The improvement is clearly visible.

Although there are some negative results, as observed in Table 1b, the overall trend is positive from the *production bed* to the *new bed* compartment. Of course, the vital point is the fact that the overall results should be positive, and it is indeed the case in this study.

Modal test results

Figure 8 illustrates the transfer function graphs for the modal test on both 'bed' compartments. The Y-axis of the graph describes the ratio of output force over input force in the unit of gravity (g = 9.81 m^2/s) over pound force (g/lb_f). If this ratio is doubly integrated, it will provide the inverse of dynamic stiffness. As shown in Figure 8 for the *new bed*, the first and second modes have higher dynamic stiffness, and also the roundness of the second mode demonstrates a higher damping ratio. The *production bed* has higher dynamic stiffness at the third mode.

Transfer function magnitude is inversely proportional to the dynamic stiffness; the smaller the magnitude, the larger the dynamic stiffness. Therefore, again in this particular case, the *new bed* is better. Table 3 gives the values of transfer function and frequency.

Another point was the frequency mismatch results between the modal test (17 Hz) and the FEA (144 Hz). In order to resolve this issue, leveling pads and screws were added to the FEA model and constraints were changed until correlation was achieved as shown in Fig. 9. After this alteration in the FEA model, it resembled the real-world model very well.

Performance Evaluation

Dynamic analysis of machine (FEA)

The two parts ‘spindle’ and ‘table’ were considered for harmonic testing. Fig. 10 shows the FEA results of harmonic testing on both *production* and *new* machines for the X-axis. The peaks show the dynamic stiffness of the two beds. The solid blue curve shows the ‘spindle,’ and the solid brown shows the ‘table’ of the *production* machine, while the dashed red and blue curves show the ‘table’ of the *new* machine. Table 3 shows the excitation frequencies of the Y and Z axes, too.

As for the *production* machine shown in Fig. 10, ‘spindle’ mode 1 is at 23 Hz, mode 2 at 37 Hz, mode 3 at 52 Hz, and mode 4 at 71 Hz. The first two modes are tool changer frequencies, which are very small on the ‘spindle.’ Nevertheless, these two modes in case of jerk motion can create a ripple or texture mark on the side wall of the test cut. Mode 3 at 52 Hz and mode 4 at 71 Hz are actual main modes of machine casting/frame, and the *new* machine should have higher dynamic stiffness than the *production* one at the above-mentioned frequencies since the dashed red curve is smaller than the solid blue curve of the *production* machine. The *production* machine ‘table’ mode 1 is at 52 Hz and mode 2 at 71 Hz. The *new* machine should have higher dynamic stiffness than the *production* machine at the frequencies mentioned above since the dashed green curve is smaller than the solid red curve of the *production* machine. Important to note that the ‘spindle’ and ‘table’ frequencies match entirely. The frequency overlap is a potential bottleneck for any machine. The excitation frequencies of other axes are presented in Table 3.

Modal (Hammer) Test on ‘spindle’ and ‘table’

This test was done on both the *production* and the *new* machines. A hammer was used to exert a force on ‘spindle’ and ‘table’ and measured the vibrations along the same axis the force was exerted. Fig. 11 illustrates the transfer function graphs for the modal test on both ‘spindle’ and ‘table.’

The *production* machine spindle’s first 3 modes occur at frequencies of 12, 16, 37, and 59 Hz at amplitudes of 1.6, 4.1, 1.3, and 1.2 x 10^{-3} g/lb_f, respectively. The *new* machine spindle’s first 4 modes occur at 11, 14, 19, 37, and 60 Hz at 1.1, 1.9, 0.9 and 1.9 x 10^{-3} g/lb_f, respectively. The values of amplitude in 3-axes for both ‘spindle’ and ‘table’ are given in Table 4.

The amplitudes of all modes of the *new* machine ‘spindle’ up to the frequency of interest (50 Hz) are smaller compared to those of the *production* machine. As it was mentioned earlier, transfer function magnitude is inversely proportional to the dynamic stiffness; the smaller the magnitude, the larger the dynamic stiffness. In Fig. 11b, it is clear that the first two modes have shorter amplitude while the third one has a higher amplitude, overall better because usually, the first two modes are the most important for machine structural stability.

Performance Verification

To verify the performance of the *new* machine, cutting test was applied under the same conditions including rpm, feed rate (in/min), and tool path, which define the final shape. In this test, the *production* and the *new* machines were used to cut identical parts, and observed the surface finish and texture

qualities of the machined parts for any differences. The final results portrayed no noticeable differences at all. It is important to note that in a simulation study, by adding ribs at suitable locations, 1.5% weight reduction was achieved (11), and in yet another study, using cross and horizontal ribs with hollow bed, the results indicated 4% weight reduction (6), but in this study, the weight reduction was 9.3% and it was experimentally verified. It was earlier mentioned that in a similar MPF simulation study, the weight of the bed was reduced by 4.8% (16).

Conclusions

We used the FEA software package to simulate weight reduction using MPF in the areas of interest while maintaining performance. We first applied the simulation to the 'bed' compartment, then extended it to the entire machine, and observed better results overall. Then, based on the simulation results, we constructed a *new* machine and tested it using the modal (hammer) test, and the test showed better results in the *new* machine as compared to the machines currently in *production*. Finally, to evaluate their cutting accuracy and precision, the same pieces were cut using both the *new* and the *production* machines, and observed no significant difference in performance; in other words, the *new* machine with 9.3% reduced weight performed just as well as the *production* machine.

Declarations

Acknowledgement

We confirm that this work is original and has not been published elsewhere, nor is it currently under consideration for publication elsewhere. The authors declare that they have no known competing financial interests or personal relationships that could have appeared to influence the work reported in this paper.

a. Funding – This research was non-financially supported by Haas Automation Inc., Oxnard, CA, USA

b. Conflicts of interest/Competing interests – There are none

c. Availability of data and material – There are none

d. Code availability – Not applicable

e. Ethics approval – Not applicable

f. Consent to participate – Not applicable

g. Consent for publication – The authors give their full consent for the publication of this article in this journal.

h. Authors' contributions – The original thought was devised by Farhad Fakour, and the manuscript preparation by Hossein Siadati. The simulation and experimentation were also conducted by Farhad Fakour.

References

1. Liu S (2015) Multi-objective optimization design method for the machine tool's structural parts based on computer-aided engineering. Int J Adv Manuf Technol 78:1053–1065. https://doi.org/10.1007/s00170-014-6700-z
2. Shen Y, Jin Y, Chu B, Luo NW, Zhu CA (2012) A multi-objective optimization method for forging machine based on genetic algorithm. China Mech Eng 23:291–294
3. Liu SH, Ye WH, Chen WF, Yang Q, Hu ZH (2010) Design plan optimum seeking of machine tool bed based on grey relational analysis. J Grey Syst 22:341–352
4. Li B, Hong J, Wang Z, Wu W, Chen Y (2012) Optimal design of machine tool bed by load bearing topology identification with weight distribution criterion. Procedia CIRP 3:626–631. . doi: 10.1016/j.procir.2012.07.107
5. Li BT, Hong J, Liu ZF (2014) Stiffness design of machine tool structures by a biologically inspired topology optimization method. Int J Mach Tool Manu 84:33–44. https://doi.org/10.1016/j.ijmachtools.2014.03.005
6. Abuthakeer SS, Mohanram PV, Kumar GM (2011)), ISSN 1584–2673Structural redesigning of a CNC lathe bed to improve its static and dynamic characteristics. Annals of Faculty Engineering Hunedoara – Int J Eng Tome IX, Fascicule 3:389–394
7. Zhao H, Sun Y, Chen R, Huang Y, Zhang G, Wang B, Mu D, Li W (2012) Static and dynamic characteristics analysis of precise composite CNC grinding machine. Adv Mater Res 411:88–93. ISSN: 1662–8985 https://doi:10.4028/www.scientific.net/AMR.411.88
8. Yang H, Zhao R, Li W, Yang C, Zhen L (2017) Static and dynamic characteristics modeling for CK61125 CNC lathe bed basing on FEM. Procedia Eng 174:489–496. https:// doi: 10.1016/j.proeng.2017.01.171
9. Duan Y, Zhang G, Guo C, Peng L, Huang Y (2011) Improvement design research of a CNC lathe-bed structure. Appl Mech Mater 50–51:1028–1032. ISSN: 1662–7482 https://doi:10.4028/www.scientific.net/AMM.50-51.1028
10. Saidaiah J, Biksham B, Veeranjaneyulu K (2017) Weight optimization of lathe bed by design modification and epoxy granite. SSRG Int J M Eng 4, 23-32 ISSN: 2348-8360
11. Swami BM, Kumar KSR (2012) Design and structural analysis of CNC vertical milling machine bed. Int J Adv Eng Tech 3:97–100. E-ISSN 0976-3945
12. Shrivastav A, Makwana D, Chelani P, Puranik P (2017) Optimization of design parameter of vertical machining center column for the weight and rigidity. Int J Adv Eng Res Dev 4:750–754

13. Srinivasan S, Subramanyam B (2016) Design and structural analysis of CNC milling machine bed with composite material. Imperial Journal of Interdisciplinary Research (IJIR) 2:147–151
14. Fakour F (1994) 'Shape optimization tool based on finite element analysis,' M.S. Thesis, California State University, Chico, USA
15. Finkelstein A (2019) Understanding mass participation factor results in frequency studies, https://www.cati.com/blog/2019/11/understanding-mass-participation-factor-results-infrequency-studies/,
16. Xu G, Sun X (2019) Study on dynamic characteristics analysis of CNC pipe thread lathe based on the energy of modal effective mass. 13:335–339
17. Irvine T (2015) Effective modal mass and modal participation factors, Revision I, http://www.vibrationdata.com/tutorials2/ModalMass.pdf,

Tables

Table 1a: Time domain; comparison of variations between the two beds for all 3 axes. The values in blue font indicate more damping

Time Domain	Left Linear Guide			Right Linear Guide		
	X	Y	Z	X	Y	Z
Production Base (g)	0.016	0.013	0.0017	0.018	0.025	0.0035
New Base (g)	0.013	0.005	0.001	0.013	0.01	0.0018
Delta (g)	0.003	0.008	0.0007	0.005	0.015	0.0017

Table 1b: Frequency domain; comparison of variations between the two beds for all 3 axes. The values in blue and red fonts indicate more damping and less damping, respectively. Important to note that the red font values show very insignificant magnitudes

Frequency Domain (FFT)	Left (FFT) at 20 Hz			Right (FFT) at 20 Hz		
	X	Y	Z	X	Y	Z
Production Base (g)	0.01130	0.00780	0.00003	0.01150	0.01200	0.00038
New Base (g)	0.00800	0.00280	0.00019	0.00840	0.00400	0.00040
Delta (g)	0.0033	0.005	-0.00016	0.0031	0.008	-0.00002

Table 2: Values of transfer function and frequency. The values in blue and red fonts indicate more damping and less damping, respectively. Important to note that the red font values show very insignificant magnitudes

Below 50 Hz Frequencies	Mode 1		Mode 2		Mode 3	
Base (Hz)	12	11	16	14	38	43
Production Base (g/lb)	0.00077		0.00187			0.00082
New Base (g/lb)		0.00071		0.00142	0.00104	

Table 3: First mode amplitude (in) for all 3 axes. The values in blue indicate more damping.

Max. up to 200 Hz	X axis	Y axis	Z axis
Production Machine 'spindle'	0.00405	0.00162	0.00300
Production Machine 'table'	0.00097	0.00060	0.00067
New Machine 'spindle'	0.00314	0.00133	0.00236
New Machine 'table'	0.00048	0.00057	0.00038

Table 4a: Values of amplitude in 3-axes for 'spindle.' The values in blue and red fonts indicate more damping and less damping, respectively. Important to note that the red font value shows very insignificant magnitudes

		Mode 1		Mode 2		Mode 3		Mode 4	
	Machine (Hz)	12	11	16	14	37	37	59	60
spindle	*Production Base (g/lb)*	0.0016		0.0041		0.0132		0.0122	
	New Base (g/lb)		0.0011		0.0019		0.0090		0.0190

Table 4b: Values of amplitude in 3-axes for 'table.' The values in blue and red fonts indicate more damping and less damping, respectively. Important to note that the red font values show very insignificant magnitudes

		Mode 1		Mode 2		Mode 3		Mode 4		Mode 5	
	Machine (Hz)	12	11	16	14	21	19	52	50	79	78
table	*Production Base (g/lb)*	0.0009		0.0032		0.0021		0.0061		0.0038	
	New Base (g/lb)		0.0005		0.0011		0.0063		0.0072		0.0038

Figures

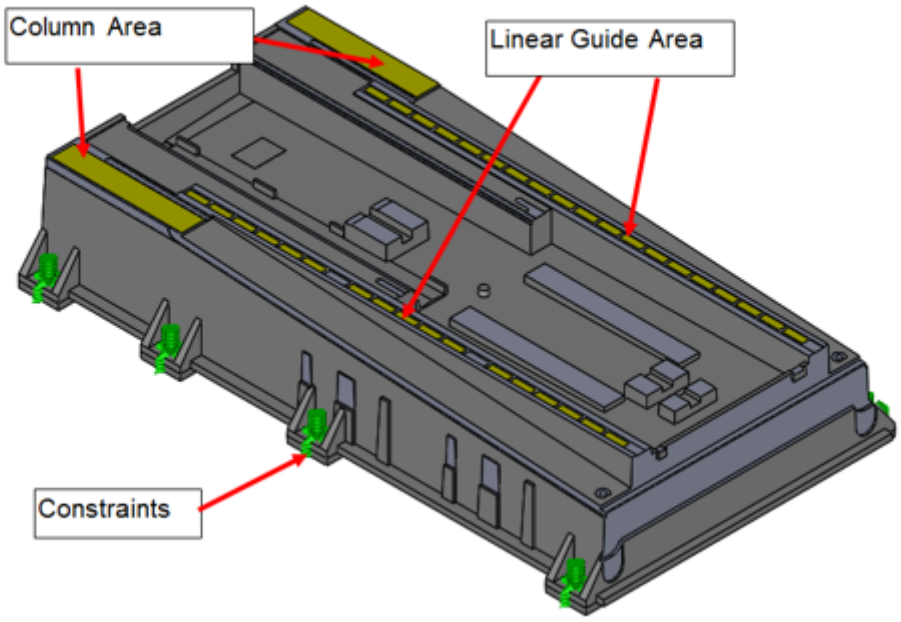

Figure 1

Starting model showing the areas of interest and the constraint sites (green color)

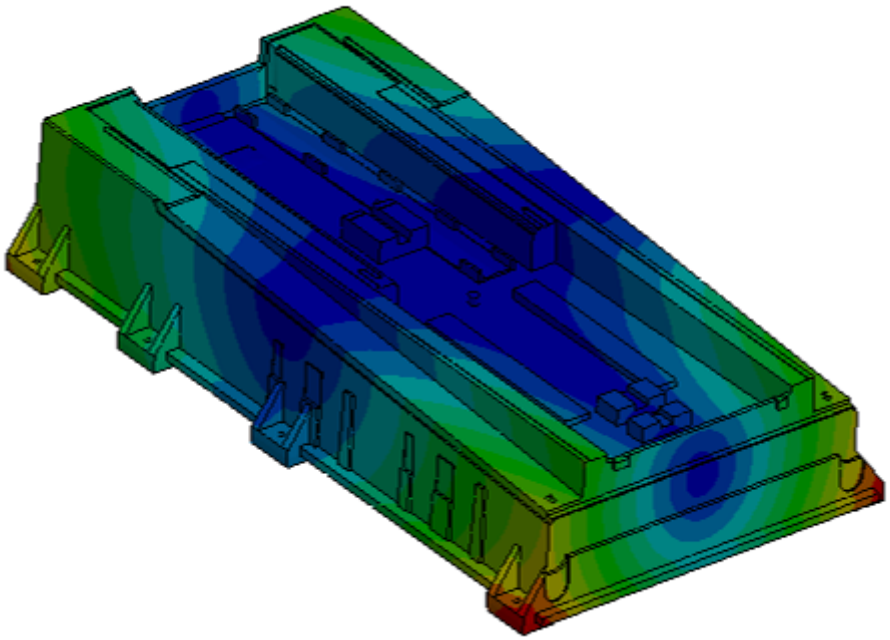

Figure 2

The bed of the production machine showing MPF in blue color

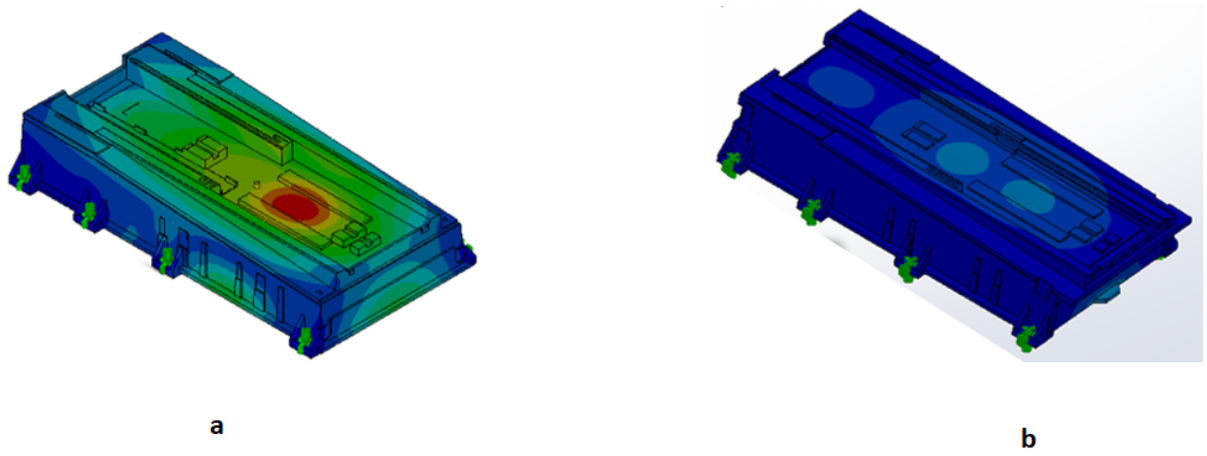

Figure 3

a: The simulated model for the production bed, for the first mode, showing constraint sites in green color
b: The simulated model for the new bed highlighting the first twisting mode in darker blue; it is superior because it has smaller amplitude

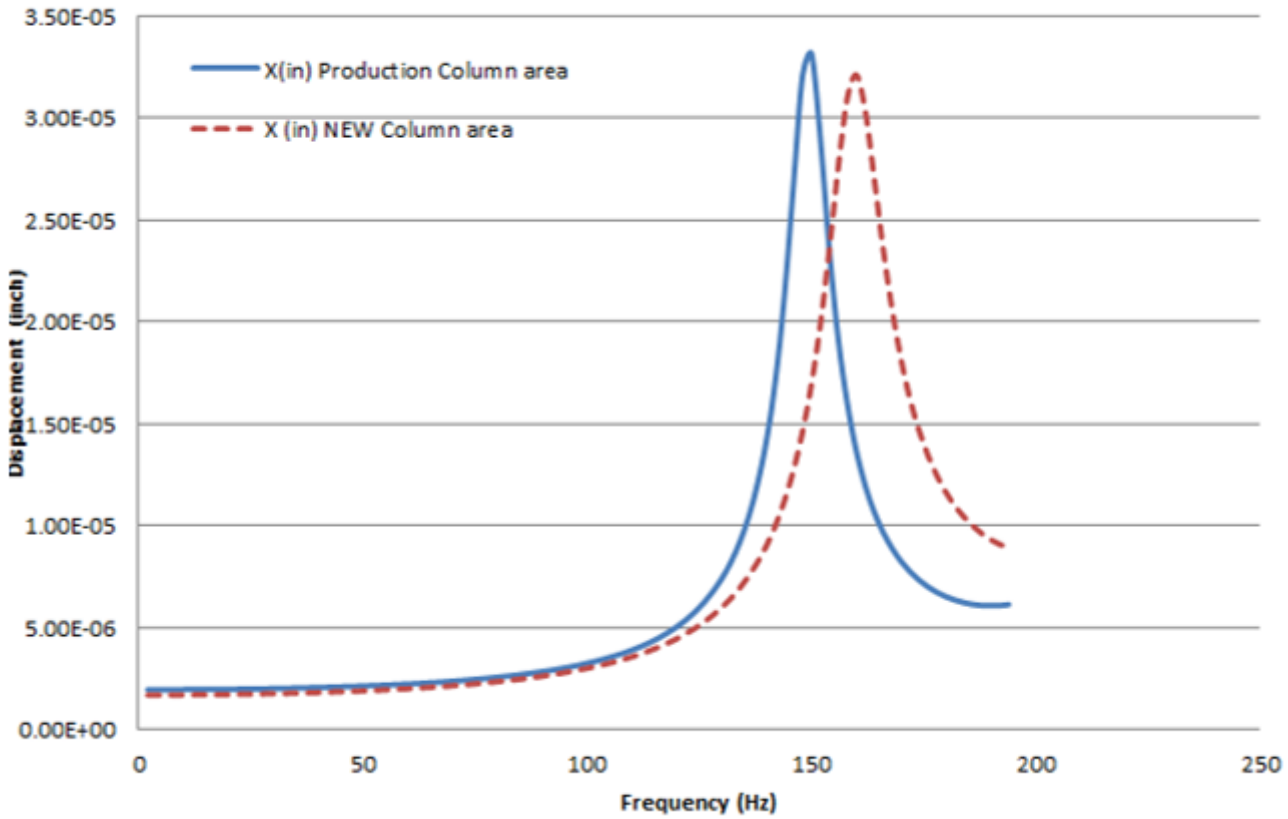

Figure 4

Comparing frequencies and amplitudes of the first modes of the production and the new models

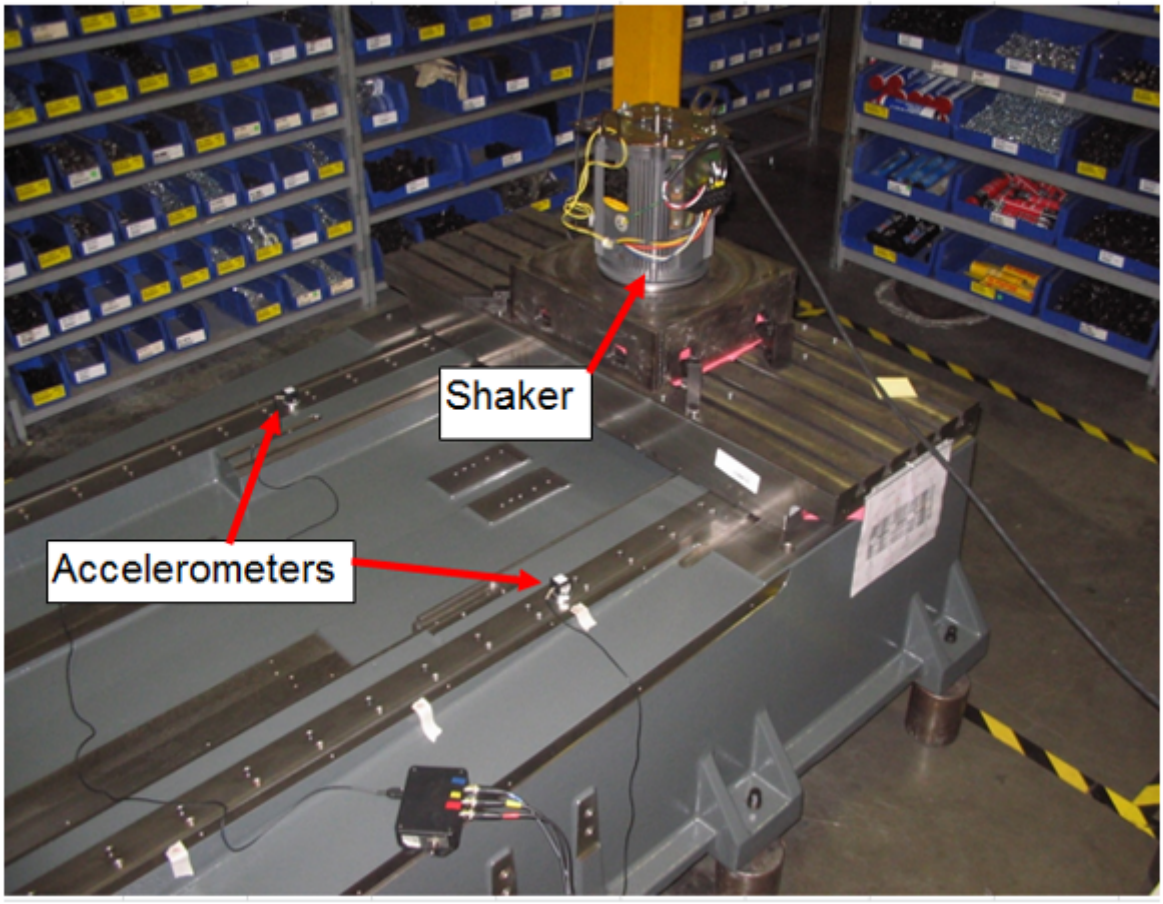

Figure 5

The ‘bed’ compartment onto which a shaker and two accelerometers (one on each left and right linear guides) were attached

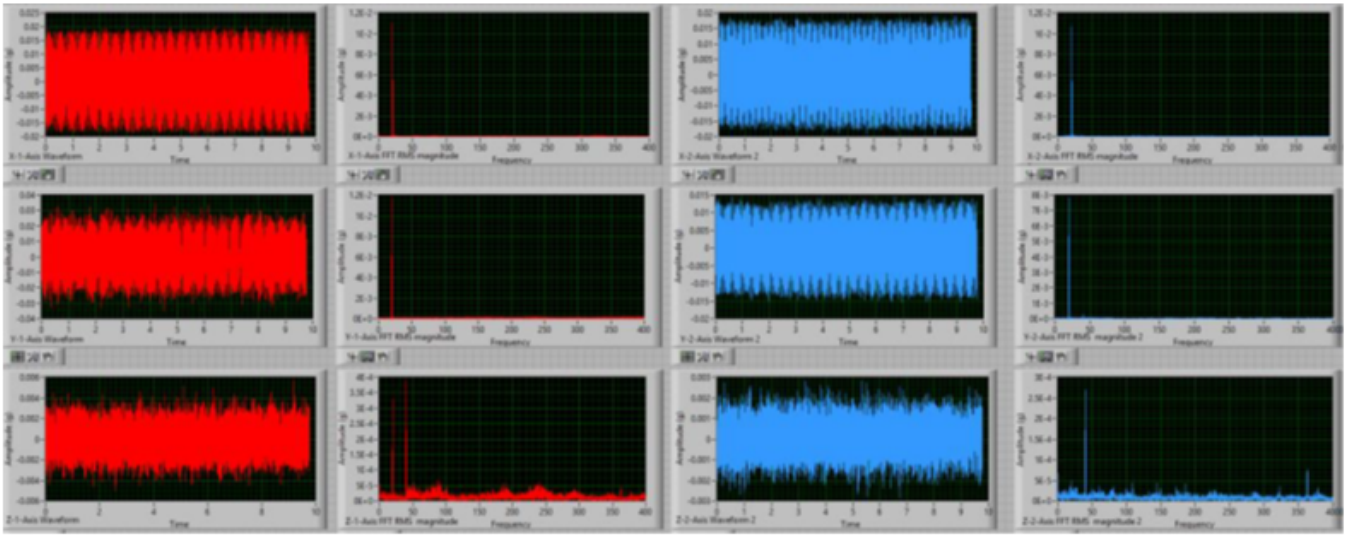

a

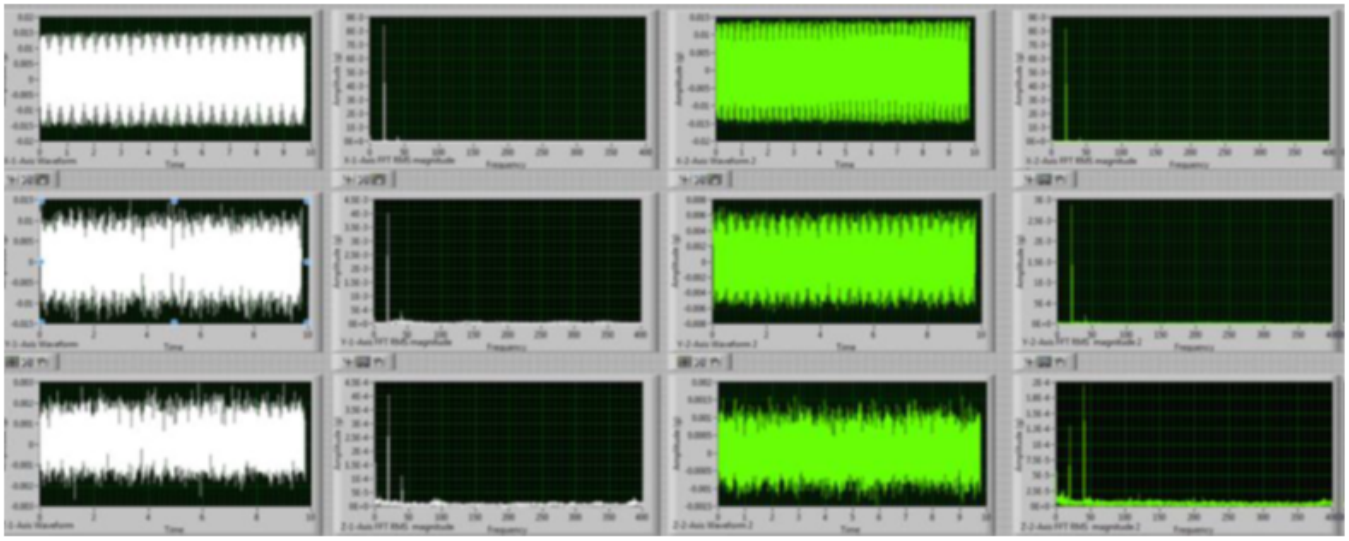

b

Figure 6

a: Vibration graphs for the production bed in all 3 axes b: Vibration graphs for the new bed in all 3 axes

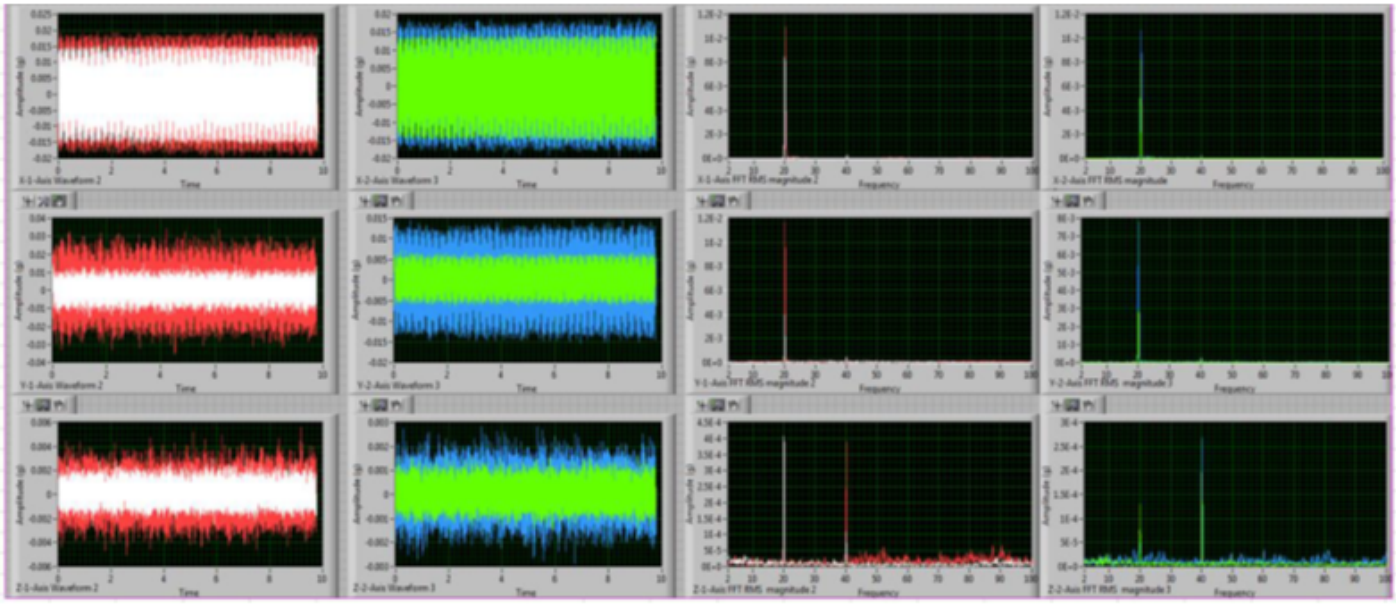

Figure 7

Variations superimposed in one graph for each side

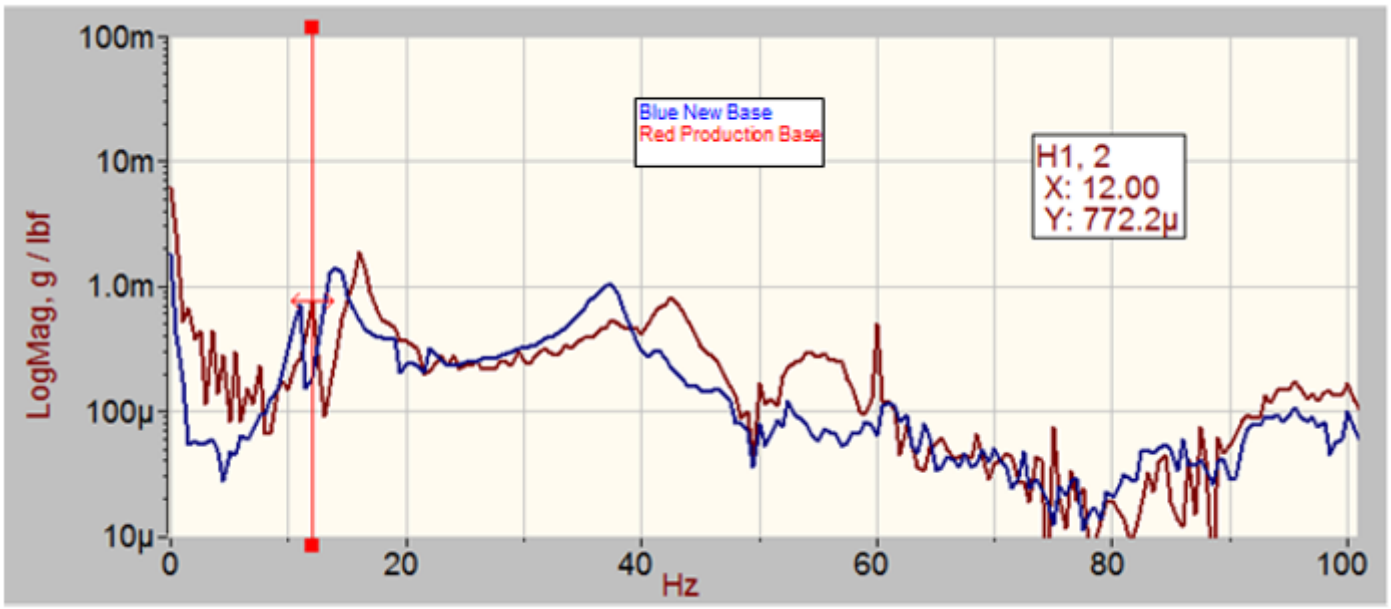

Figure 8

Transfer function graphs for the modal test on both ‘bed’ compartments

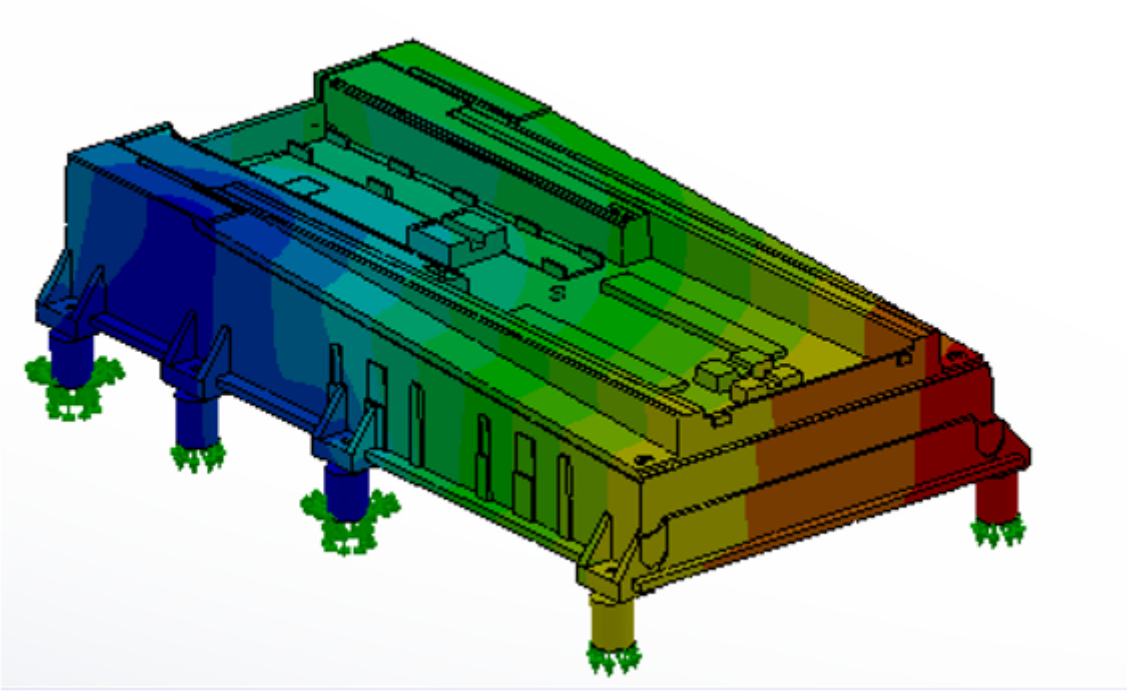

Figure 9

Correlation was achieved after changing constraints

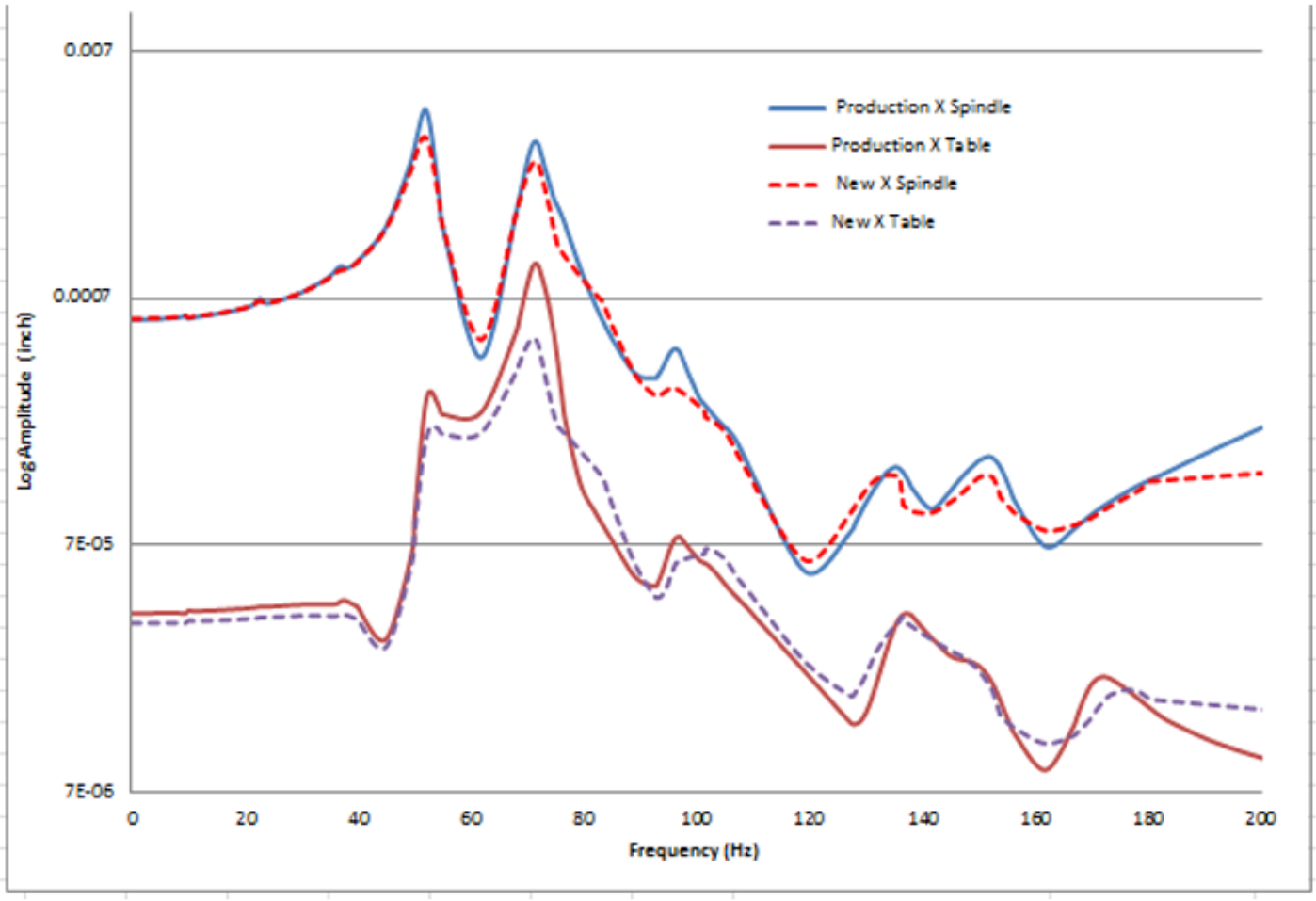

Figure 10

FEA results of harmonic testing on both production and new machines, X-axis

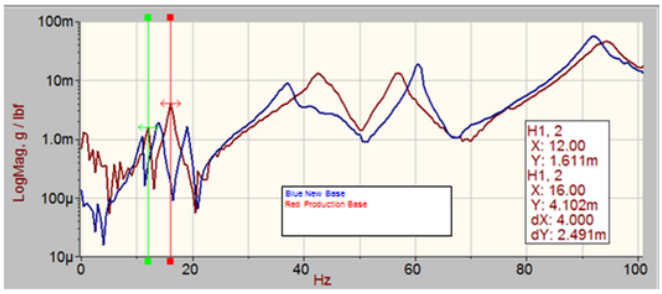

a

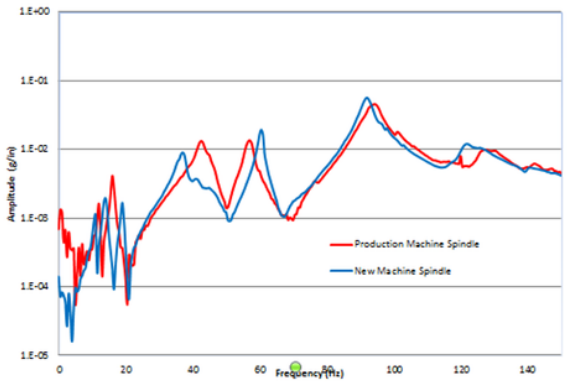

b

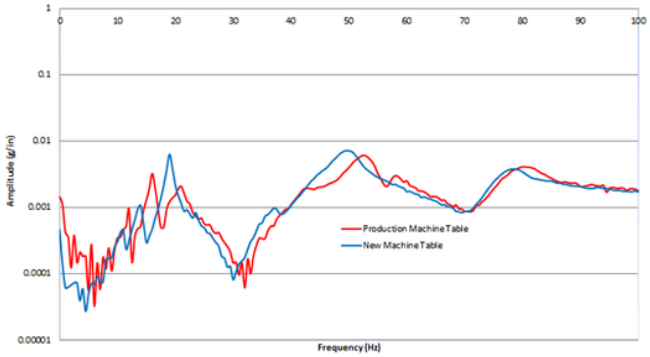

c

Figure 11

a: Transfer function graphs for modal tests from Data Physics for both production bed and new bed b: Transfer function graphs for the modal test on ‘spindle’ c: Transfer function graphs for the modal test on ‘table’